International Journal of Research in Engineering and Science (IJRES)
ISSN (Online): 2320-9364, ISSN (Print): 2320-9356
www.ijres.org Volume 10 Issue 3 ǁ 2022 ǁ PP. 31-37

Experimental determination of the phase diagram of Al-Si alloysunderreal casting conditions.

Adefuye, O. A.[1], Fadipe, O. L.[1], Orisaleye, J. I.[2], Adedeji, K.A.[1]*
[1]*Department of Mechanical Engineering, Faculty of Engineering, Lagos State University-Epe Campus*
[2]*Department of Mechanical Engineering, Faculty of Engineering, University of Lagos, Akoka, Nigeria.*

ABSTRACT
Solidification is an essential step of heat exchange which occurs between the casting,the mold and the environment.The knowledge of the solidification process is important for the control of variables to ensure castings attain required specifications Phase diagrams reveal a lot about solidification, giving the composition and quantity of the phases in equilibrium with each other at any temperature Most of the phase diagrams (determined either experimentally or fromestimations) are equilibrium phase diagrams.They are therefore true for equilibrium states which are very often very far from usual casting states. In this study, a method is developed tor accurate determination of the nonequilibrium phase diagram of super pure Al-Si alloysunder normal casting conditions.
Keywords: *Non-equilibrium phase diagram, solidification end point, super pure Al-Si alloys, cooling curves.*

Date of Submission: 28-02-2022 Date of acceptance: 09-03-2022

I. INTRODUCTION

Casting has a very important economic impact. To have a successful setup and tight control on the casting process, an in-depth knowledge of the process technological windows is a first requirement (Gonzalez et al., 2003). Adefuye et al. (2019; 2020) noted that the capability of foundries can be improved with increased knowledge of foundry processes. It is important to ensure that variables can be controlled to meet required specifications.During casting processes, solidification is considered to be a very essential step of heat exchange which occurs between the casting, the mold and the environment. Solidification determines the microstructure and the properties of the cast (Wladysiak, 2013).Chattopadhyay (2011) noted that the estimation of solidification time is a first-hand requirement at the shop floor.

There have been several studies on casting and particularly the solidification behaviour of castings. Ji et al. (2013) investigated the microstructural evolution and solidification behaviour of Al-Mg-Si alloy in high-pressure die casting and observed that solidification commences with the formation of primary α-Al phase in the shot sleeve and is completed in the die cavity.Muojekwu et al. (1995) studied the transient heat transfer in the early stages of solidification of Al-Si alloy on a water-cooled chill and the consequent evolution of microstructure. It was noted that the secondary dendrite arm spacing was dependent on cooling rate and local solidification time along with the heat transfer coefficient at distances very near the casting/chill interface.Adefuye et al. (2021a; 2021b) studied the fluidity of Al-Si alloys in a fluidity test channel and noted that the mode of solidification may be the most important factor affecting fluidity.

Tu et al. (2012) predicted the position of the solidification end point during continuous casting using a software. It was noted that the casting temperature had little effect on the solidification end point but the solidification end point moved backward significantly with increase in casting speed. Chattopadhyay (2011) reported on the solidification time of simple shaped molds using a finite volume numerical computation. Mohanty and Sarangi (2020) noted that alloys can be classified into three categories based on solidification process. These include alloys with narrow freezing zone which freeze with marked skin formation, alloys with long feeding ranges where solidification proceeds simultaneously in much of the casting, and alloys which show expansion on freezing.

The phase diagram is a graphical representation of the domain in which a given state is possible.Phase diagrams are very important in various aspects of metallurgy, especiallyin physical metallurgy and heat treatment. The diagrams are determined either theoretically or experimentally to generate cooling curves for the different alloys on the system. A reliable phase diagram information is essential for understanding the transformation in solidification (Xu et al., 2017). Xu et al. (2017) investigated the correlation between the cooling curves and solidification behaviour of a hypereutectic alloy of Fe-B. Gao et al. (2019) studied the microstructure and solidification behaviour of a nickel-based superalloy at different cooling rates.

Thermal analysis of the cooling curves is carried out to determine points at which phase transformation occurs and the points at which all transformation ends. It is a classical method for the determination of phase diagrams (Fredriksson, 1988). The nucleation points which give rise to the liquidus were relatively easy to determine.The end of solidification points which give rise to the solidus was more difficult to determine (Chalmers, 1970). Early works in this field are mainly concerned with transformation at equilibrium or near equilibrium conditions. Most industrial processes take place under non equilibrium conditions.Analysis of cooling curves obtained under industrial conditions is also beneficial.Liang et al. (2008) carried out a study on the thermal analysis and solidification pathways of Mg-Al-Ca system alloys and noted that the analysis of cooling curves will lead to better understanding of the formation of cast microstructures and defects. This work presents a study on the non-equilibrium solidification of super pure Al-Si alloys.

Theory

The analysis of cooling curve is based on the thermal events that occurred during phase transformation.When a solid phase is nucleated, the liberation of the latent heat of solidification slows down the cooling of the material.At the end of solidification, the release of latent heat stops.Also, all the material is all solid and heat transfer is entirely by conduction. The last liquid to solidify does so very quickly and the heat liberated is conducted away very rapidly (Chalmers, 1970). It is also the end of phase transformation andhence, the last thermal event during solidification.

Nucleation points are quite visible on the cooling curve they occur at turning points.Solidification end point occurs as points of inflection on the cooling curve. The inflection occurs over a short period of time (less than one second)and is better located by the second derivative as illustrated in Figure 1, (Adefuye, 1997).

The use of analog /digital converter devices and computers have led to automated rapid logging of data and fuller cooling curves. Using these devices, it is a simple matter to plot and analyze the cooling curves. Analysis of cooling curves may be used to predict a variety of properties such as percentage of a phase in the liquid, the extent of modification of silicon eutectic and the extent of grain refinement.

The methods in use can be classified into two, the ones that involve the use of the zero curve (or baseline curve), and those that don't. The baseline is the first derivative of the cooling curve assuming no heat was released during solidification. The zero curve has to be calculated.Any deviation of the first derivative of the cooling curve from the zero curve signifies a solidification event has taken place at the point. The accuracy of this methoddepends on the accuracy of the calculated zero curve.

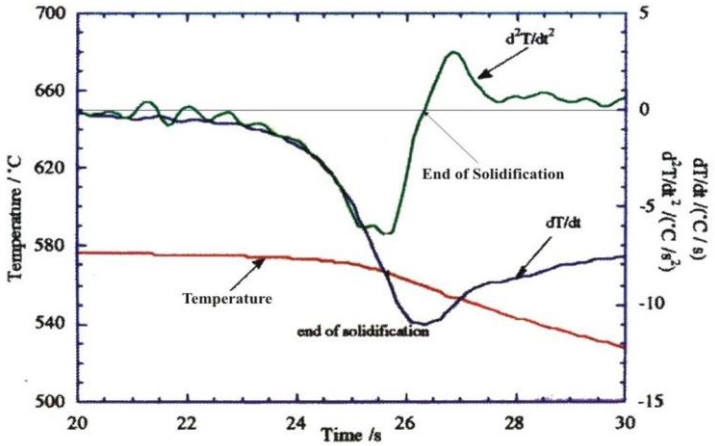

Figure 1: Cooling curve analysis using the first derivative and second derivative to determine the solidification end point.

The other method is to take the last minimum on the first derivative as the solidification end point. As illustrated in Figure 1. The second derivative isbased on the observation that the solidification end point manifests as an inflection in the temperature time curve.Hence, the solidification end point occurs at the point the second derivative equals zero. The minimum on the first derivative corresponds to zero on the second derivative the temperature at this point is then taken as the solidification end point.

II. Experimental Methods

The alloys were made from aluminum of 99.999% purity and silicon that was 99.9999% pure. The silicon content of the alloys that were investigated was, 0.5%, 1%, 1.5%, 2%, 4%, 6%, 8%, 10%, 11%, 12%, 13%, 14%, 15%, 16%, 17%, 18%, 19%, and 20%. The pattern used to produce the mold is illustrated in Figure

2.Each of the channels was 20 mm wide and the depth varied from 8 mm to 0.5mm.The mold was produced using silica sand of size AFS 60 bonded by '*pepset'* according to standard procedures.

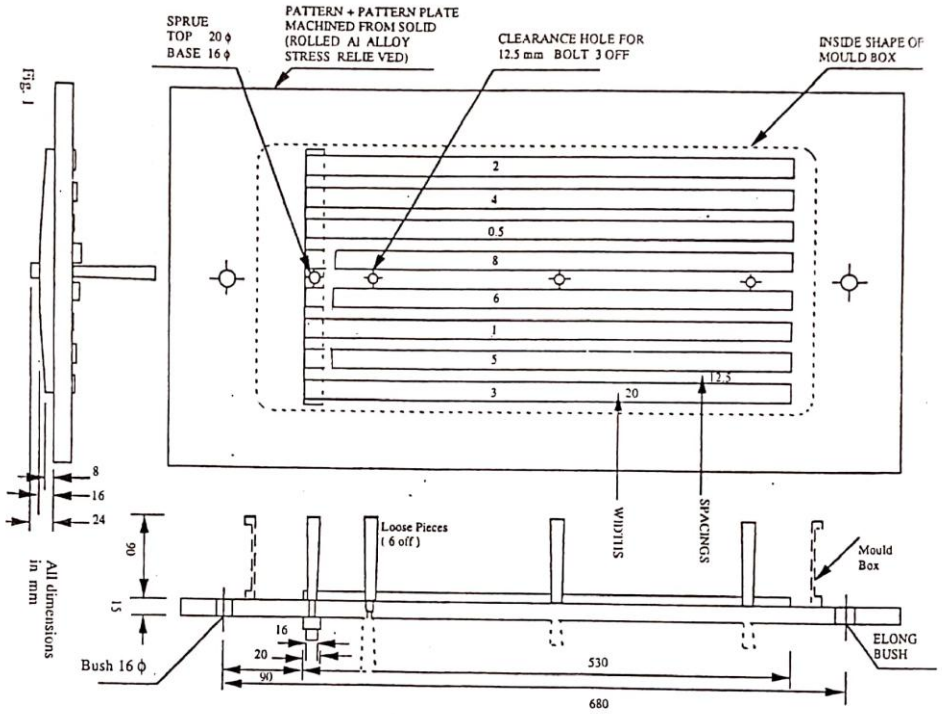

Figure2: Pattern used to prepare the mold.

Thermocoupleswere made by spot welding of crossed wires of glass fiber wrapped 0.3mm thick K-type thermocouple wires. TheK-type thermocouple wires were located as centrally as possible in the geometric center of the channel at a point 7mm from the inlet.The EMFsignal from the thermocouple was amplified to a signal in the range 0 to 5V (corresponding to -100^0C to 1350^0C). The signal was converted to a digital signal and logged into a file by a temperature logger a program written in the *labview*graphical programming environment.The analog to digital signal converter has an acquisition error corresponding to $\pm 0.35^0$C.

Acquisition of data was started some seconds before pouring. The data acquisition rate was 50 readings per second.Data was acquired for 250 seconds by which time the channel had completely solidified. Pouring temperature for all alloys was 750^0C except the Al-20%Si which was poured at 800^0C.

Within the temperature range of 550°C and750°C k-type thermocouples are accurate to±5°C (Kollie et al., 1975).Therefore, some of the recorded temperatures were $\pm 5^0$C outside their real values and constituted noises on the cooling curve.The data was smoothed by carrying out a five-point compressed average on it followed by an eleven-point running average. The smoothed data was then differentiated once to yield the first derivative and again to yield the second derivative from which the solidification end point was determined.

Derivatives were calculated using a convolution algorithm derived by Savistky and Golay(1964). Convolution parameters which fitted for a fourth order polynomial curve to 9 data points and calculated the first derivative at the fifth point were used in a macro program.

III. Results and discussion

The cooling curveused in the determination oftransformation points of Al-1%Si alloy is shown in Figure 3. Figures 4 to 6 show the cooling curves for Al-8%Si, Al-13%Si and Al-20%Si, respectively.

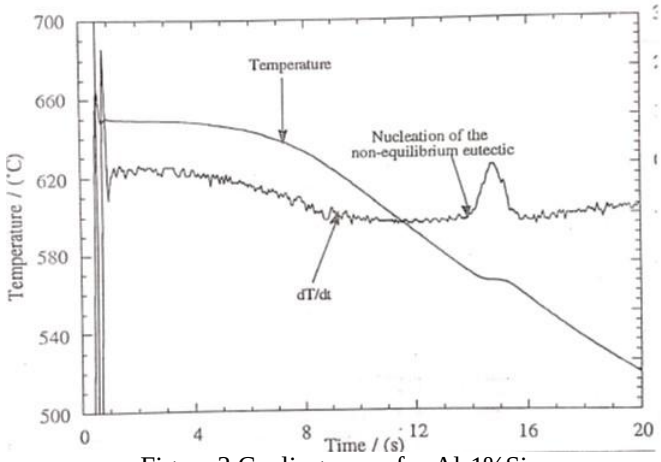

Figure 3:Cooling curve for Al-1%Si

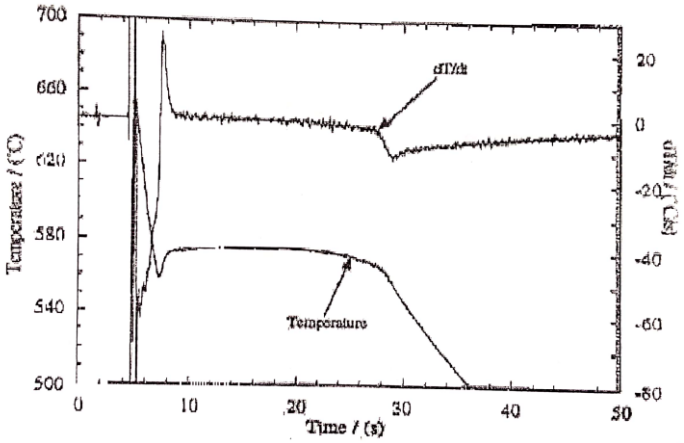

Figure 4:Cooling curve of Al-8%Si alloy

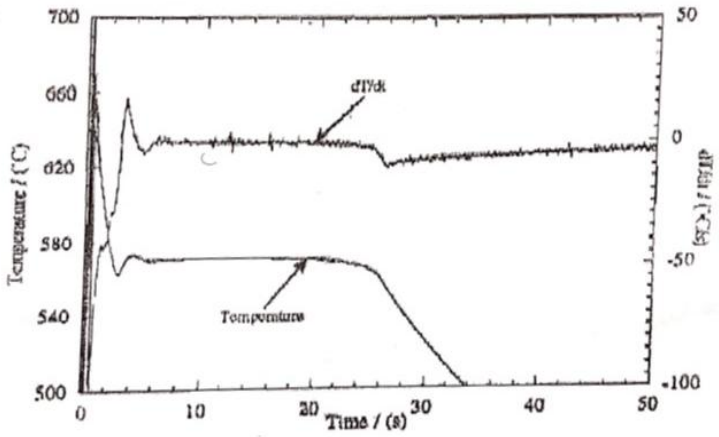

Figure 5: Cooling curve of Al-13%Si alloy

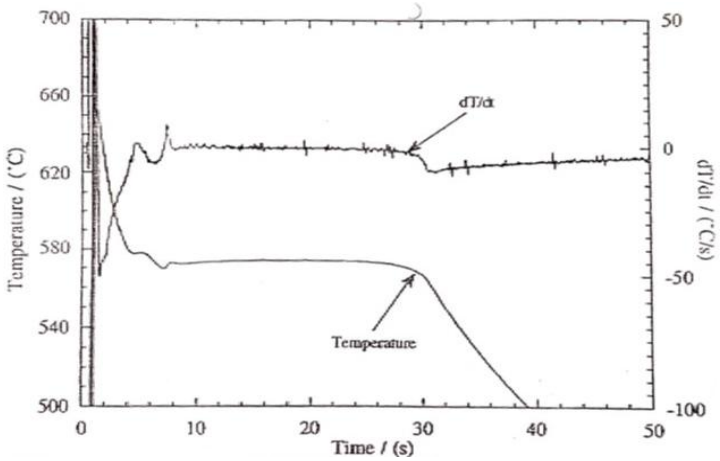

Figure 8:Cooling curve of Al-20%Si

Figure 9shows a micrograph of the Al-0.5%Si alloy specimen illustrating the eutectic.The presence of the eutectic in this solid solution alloy is an indication of how far away from the equilibrium the operation was carried out.

Figure 10 shows the non-equilibrium phase diagram super imposed on the liquidus of the equilibrium phase diagram.For all materials, it is observed thatthe liquidus of the non-equilibrium phase diagram is lower than that of the equilibrium phase diagram. The liquidus temperature decreased linearly with increasing silicon content up to a silicon content of 13% as previously observed by Penget al.(2017). Between a silicon content of 13% and 20% the liquidus temperature increased with increasing silicon content, the observation of Peng et al (2017) that at the Al-18%Si, the only hypereutectic alloy they worked on, the liquidus temperature increased greatly. On the pure aluminium and thehypoeutectic alloys side of the diagram where the primary phase is aluminium, the difference between the liquidus temperature on the non–equilibrium phase diagram and the equilibrium phase diagram vary from 10°C for Al-1%Si to 25°C for Al-12%Si.On the hyper-eutectic part of the diagram, where silicon is generally the primary phase, the difference between the liquidus temperature on the non-equilibrium phase diagram and that of the equilibrium phase diagram the temperature difference varies from 25°C at Al-13%Si to 170°C at Al-20%Si. This huge difference is attributable to the difference in the latent heat of fusion of the primary phases. The latent heat of fusion of aluminium is 386.9 kJ/kg while the latent heat of fusion of silicon is 1,809 kJ/kg (Ross, 2013).

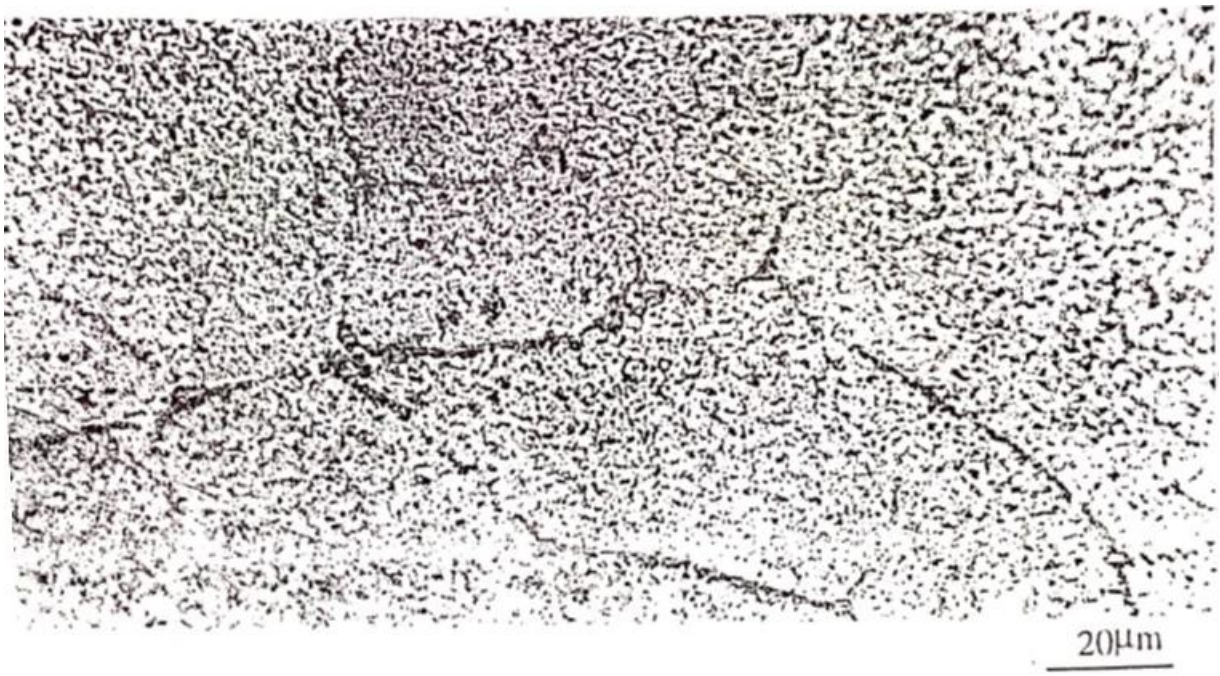

Figure 9 micrograph of Al-0.5 %Si showing the eutectic structure

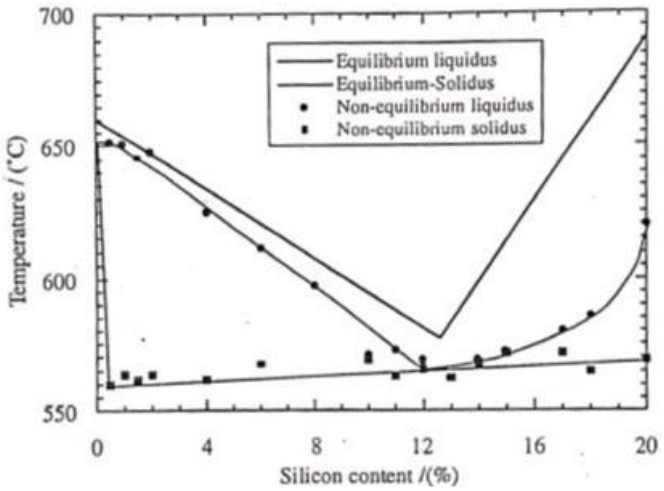

Figure 10: Non-equilibrium phase diagram of the super-pure alloys superposed on the equilibrium diagram of Al-Si alloys

IV. Conclusion

Most of the phase diagrams, determined either experimentally or fromestimations, are equilibrium phase diagrams.They are therefore true for equilibrium states which are very often very far from usual casting states. In this study, a method is developed tor accurate determination of the non-equilibrium phase diagram of super pure Al-Si alloys under normal casting conditions. From this study, it was found that the liquidus of the non-equilibrium phase diagram is lower than that of the equilibrium phase diagramfor all materials. Ahuge difference was observed between the liquidus temperature,which varies from 25°C at Al-13%Si to 170°C at Al-20%Si, on the hypereutectic part of the non-equilibrium phase diagram and the equilibrium phase diagram. This large difference was attributed to the difference in the latent heat of fusion of the primary phases.

Acknowledgement

We wish to thank the Association of Commonwealth Universities for sponsoring this work.

References

[1]. Adefuye, O, Orisaleye, J., Fadipe, O., and Adedeji, K. (2021a). The effect of grain refinement of primary aluminum on the fluidity of Al-Si casting alloys. Chemistry and Materials Research, 13(1):36-42.
[2]. Adefuye, O. A., Fadipe, O. L., Adedeji, K. A., and Orisaleye, J. I. (2021b). The effect of grain refining of primary silicon on the fluidity of Al-Si casting alloy. International Journal of Engineering Applied Science and Technology, 5(9): 71-75.
[3]. Adefuye, O. A., Orisaleye, J. I., Lawal, O. I., and Fadipe, O. L. (2020). Gating system design solutions for casting defects from pouring. Engineering and Technology Research Journal, 5(1):26-31.
[4]. Adefuye, O. A., Orisaleye, J. I., Lawal, O. I., and Fadipe, O. L. (2019). Gating practices in Nigerian research and training institutes: case study of Lagos state. Journal of Physics: Conference Series, 1378(3):032095.
[5]. Adefuye, O. A. (1997). The fluidity of Al-Si casting alloys. Phd thesis, University of Birmingham. U.K.
[6]. Chalmers, B. (1970). Principles of Solidification. Applied Solid State Physics, 161–170.
[7]. Chattopadhyay, H. (2011). Estimation of solidification time in investment casting process. The International Journal of Advanced Manufacturing Technology, 55(1-4):35-38.
[8]. Fredriksson, H. (1988). Interpretation and use of cooling curves (thermal analysis). *ASM Handbook.*, *15*, 182-185.
[9]. Gao, B., Sui, Y., Wang, H., Zou, C., Wei, Z., Wang, R., and Sun, Y. (2019). Effects of cooling rate on the solidification and microstructure of nickel-based superalloy GTD222. Materials, 12:1920.
[10]. Gonzalez, M., Goldschmit, M. B., Assanelli, A. P., Berdaguer, E. F., and Dvorkin, E. N. (2003). Modelling of the solidification process in a continuous casting installation for steel slabs. Metallurgical and Materials Transactions B, 34B: 455-473.
[11]. Ji, S., Wang, Y., Watson, D., and Fan, Z. (2013). Microstructural evolution and solidification behaviour of Al-Mg-Si alloy in high-pressure die casting. Metallurgical and Materials Transactions A, 44A:3185-3197.
[12]. Kollie, T. G., Horton, J. L., Carr, K. R., Herskovitz, M. B., and Mossman, C. A. (1975). Temperature measurement errors with type K (Chromel vs Alumel) thermocouples due to short-ranged ordering in Chromel. *Review of Scientific Instruments*, *46*(11), 1447-1461.
[13]. Liang, S. M., Chen, R. S., Blandin, J. J., Suery, M., and Han, E. H. (2008). Thermal analysis and solidification pathways of Mg-Al-Ca system alloys. Material Science and Engineering A, 480:365-372.
[14]. Mohanty, U. K., and Sarangi, H. (2020). Solidification of metals and alloys. In: Casting Processes and Modelling of Metallic Materials, Chapter 2, https://doi.org/10.5772/intechopen.91879.
[15]. Muojekwu, C. A., Samarasekera, I. V., and Brimacombe, J. K. (1995). Heat transfer and microstructure during the early stages of metal solidification. Metallurgical and Materials Transactions B, 26: 361.
[16]. Peng, T., Zhiliu, H.,Yanjun,Z. and Qingbao, H. (2017). Investigation on the solidification course of Al-Si alloys by using a numerical Newtonian thermal analysis method *Mater. Res. Express* in press https://doi.org/10.1088/2053-1591/aa9cf6. 12.
[17]. Ross, R. B. (2013). Metallic materials specification handbook. Springer Science & Business Media, UK.
[18]. Savitzky, A. andGolay, M. J. (1964). Smoothing and differentiation of data by simplified least squares procedures. *Analytical chemistry*, *36*(8), 1627-1639.

[19]. Tu, T., Wang, H., Lei, Z., and Ren, Z. (2012). Prediction of the position on solidification end point of continuous caster. Advanced Materials Research, 421: 67-70.
[20]. Wladysiak, R. (2013). Computer control the cooling process in permanent mold casting of Al-Si alloy. Archives of Metallurgical and Materials, 58(3):977-981.
[21]. Xu, J., Jian, Z., Dang, B., Zhang, D., and Liu, F. (2017). Solidification behavior and cooling curves for hypereutectic Fe-21 At. Pct B alloy. Metallurgical and Materials Transactions A, 48(4), 1817–1826.